PROCEEDINGS, Fourteenth Workshop on Geothermal Reservoir Engineering
Stanford University, Stanford, California, January 24-26, 1989
SGP-TR-122

COMPARISON OF PRESSURE TRANSIENT RESPONSE IN INTENSELY AND SPARSELY FRACTURED RESERVOIRS

Johns, R.T. and Jalali-Yazdi, Y.

Stanford University

ABSTRACT

A comprehensive analytical model is presented to study the pressure transient behavior of a naturally fractured reservoir with a continuous matrix block size distribution. Geologically realistic probability density functions of matrix block size are used to represent reservoirs of varying fracture intensity and varying degrees of fracture uniformity. Transient interporosity flow is assumed and interporosity skin is incorporated.

Drawdown and interference pressure transient tests are investigated. The results show distinctions in the pressure response from intensely and sparsely fractured reservoirs in the absence of interporosity skin. The pressure response in a nonuniformly fractured reservoir approaches that of a nonfractured (homogeneous) reservoir for the case of large matrix block size variability. Type curves are developed to estimate matrix block size variability and the degree of fracture intensity for drawdown and interference well tests.

INTRODUCTION

Currently, matrix block size distribution is not considered a determinable parameter from pressure transient tests. Yet, the utility of determining matrix block size distributions is paramount since block size is one of the main parameters of a fractured reservoir that governs producibility. In one phase flow, it controls the transition from early production from the fractures to late production from the total reservoir (matrix and fractures). In two phase flow, it controls the rate of imbibition (or displacement) and ultimately the recovery efficiency of the reservoir[11].

The Warren and Root model [19] and other pressure transient models of naturally fractured reservoirs assume fracture intensity is constant throughout the reservoir, i.e., they assume fracturing is uniform and matrix block size is constant. Geological and geomechanical studies of fractured reservoirs and outcrops, however, commonly report occurrences of nonuniform fracture patterns due to variability in lithology, bed thickness, degree of diagenesis, and stress environment [1,3,8,16,18,12,9]. For reservoir engineering purposes, fracture patterns can be represented by simple geometric shapes or designs shown in Figure 1. Skewed fracture patterns can also result due to variability in matrix block size and intersection angle.

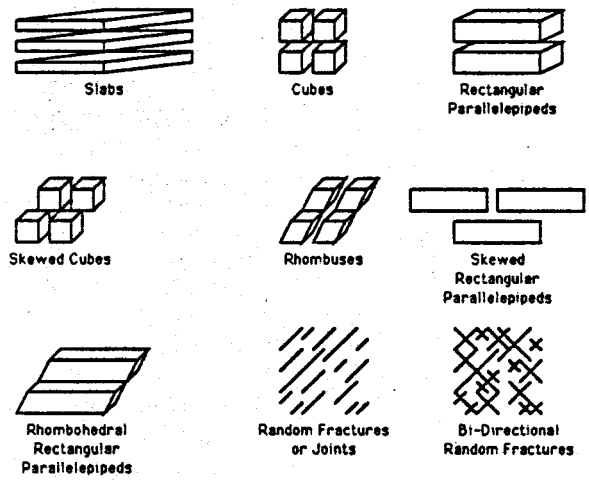

Figure 1: Idealizations of Typical Fracture Patterns seen in Nature.

Some fractures are calcite cemented or mineral filled which can restrict flow from the matrix blocks to the fractures. This phenomenon can be included as interporosity skin.

The distribution of fracture lengths commonly observed in outcrops are exponentially decaying (i.e. there are many short joint lengths and few large joint lengths). Figure 2 illustrates a probability density function constructed from an outcrop in the Mt. Abott quadrangle of the central Sierra Nevadas [18].

In well testing literature, the variability of matrix block size is generally not considered and a pseudosteady state (PSS) interporosity flow assumption is commonly used. Cinco-Ley *et al* [5], however, used a discrete model of up to five different block sizes and demonstrated the transition zone is affected significantly while the late and early time responses are not. Both Cinco-Ley *et al* , and Moench [13] presented a realistic explanation for the observance of the PSS behavior by introducing an interporosity skin factor. Belani and Jalali-Yazdi [2] extended the discrete formulation of Cinco-Ley *et al* to continuous probability density functions of matrix block size. They considered three probability density functions: Dirac delta, uniform, and bimodal. With an increase in the variance of the matrix block size distribution, they found features of a fractured reservoir response become less pronounced.

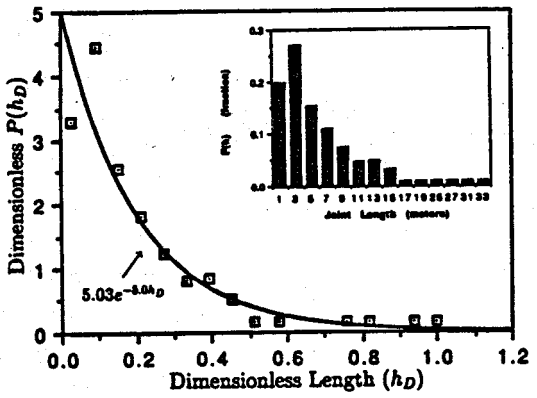

Figure 2: Construction of Probability Density Function from Outcrop, Central Sierra Nevadas.

In this paper, a continuous probability density function of matrix block sizes will be used. The objective is to show that drawdown and interference well testing can provide an indication of the degree of fracture intensity and the degree of uniformity of fracturing.

THEORY AND SOLUTION

The diffusivity equation for a double porosity reservoir can be modified to include a random distribution of matrix block size by adding a source integral [2]:

$$\frac{k_f}{\mu}\nabla^2 P_f = \phi_f c_f \frac{\partial P_f}{\partial t} + \int_{h_{min}}^{h_{max}} Q(h)P(h)\,dh. \quad (1)$$

The source integral in Equation 1 accounts for the flow contribution of the matrix to the fracture. It is assumed that fluid travels from the matrix to the fractures and to the wellbore. P(h) is the probability density function (PDF)describing the likelihood of a certain matrix block size to exist and Q(h) is the flow contribution from that matrix block to the fracture. For transient interporosity flow and slab geometry:

$$Q(h) = -\frac{k_m}{\mu h}\nabla p_m\,|_{interface}\,. \quad (2)$$

Q(h), therefore, takes into consideration the mode of interporosity flow and also the geometry of the matrix blocks.

For a well producing at constant rate in an infinite reservoir, the interference solution in Laplace space is:

$$\overline{P}_{D_f} = \frac{K_0(x r_D)}{s[C_D s(K_0(x) + S_D x K_1(x)) + x K_1(x)]}, \quad (3)$$

and for drawdown:

$$\overline{P}_{D_w} = \frac{K_0(x) + S_D x K_1(x)}{s[C_D s(K_0(x) + S_D x K_1(x)) + x K_1(x)]}. \quad (4)$$

Parameter s is the Laplace variable related to dimensionless time (t_D) and the Bessel function argument is:

$$x = \sqrt{sf(s)}. \quad (5)$$

The function f(s) embodies the reservoir parameters including the matrix block size distribution. For transient interporosity flow in the presence of interporosity skin:

$$f(s) = \omega_f + \omega_m \int_{h_{ratio}}^{1} \frac{\sqrt{\frac{\lambda}{\omega_m s}}\tanh(\sqrt{\frac{\omega_m s}{\lambda}})P(h_D)}{1 + S_{ID}\sqrt{\frac{\omega_m s}{\lambda}}tanh(\sqrt{\frac{\omega_m s}{\lambda}})}dh_D, \quad (6)$$

where,

$$h_{ratio} = \frac{h_{min}}{h_{max}}, \quad (7)$$

$$S_{ID} = \frac{k_m h_s}{k_s h}. \quad (8)$$

The interporosity skin factor (S_{ID}) is a function of matrix block size distribution and, hence is only constant when $\frac{h_s}{\lambda}$ is constant. A more realistic assumption is that the depth of skin damage (h_s) is constant for all matrix blocks, and hence, S_{ID} can be defined as:

$$S_{ID} = S_{ID_{min}}\sqrt{\frac{\lambda}{\lambda_{min}}}, \quad (9)$$

where,

$$S_{ID_{min}} = \frac{k_m h_s}{k_s h_{max}}. \quad (10)$$

and now:

$$f(s) = \omega_f + \omega_m \int_{h_{ratio}}^{1} \frac{\sqrt{\frac{\lambda}{\omega_m s}}\tanh(\sqrt{\frac{\omega_m s}{\lambda}})P(h_D)}{1 + S_{ID_{min}}\sqrt{\frac{\omega_m s}{\lambda_{max}}}tanh(\sqrt{\frac{\omega_m s}{\lambda}})}dh_D. \quad (11)$$

PROBABILITY DENSITY FUNCTIONS

Prediction of the pressure response requires the type of matrix block size distribution be known or assumed. Once the PDF is selected, fracture intensity can then be inferred from pressure transient data. Two types of probability density functions are used to represent the variability of matrix block sizes. These types, exponential and linear (Figure 3), occur most often as indicated in the geological literature. The Dirac delta (or uniform block size) and rectangular distribution are each subsets of the exponential and linear distributions. As fracture intensity increases, mean block size decreases and P(h) becomes skewed to the smaller block sizes. As fracture intensity decreases, the reverse is true.

The exponential PDF is given by:

$$P(h_D) = \frac{a(exp^{-ah_D})}{exp^{-(ah_{ratio})} - exp^{-a}}, \quad (12)$$

where 'a' is the exponential constant. The linear distribution function is:

$$P(h_D) = \frac{mh_D + b}{.5m(1 - h_{ratio}^2) + b(1 - h_{ratio})}, \quad (13)$$

where 'm' is the slope and 'b' is the vertical intercept of the cartesian plot of $P(h_D)$ versus h_D. Because a probability function must be positive, the slope must be in the range:

$$\frac{-2}{(1 - h_{ratio})^2} \le m \le \frac{2}{(1 - h_{ratio})^2}. \quad (14)$$

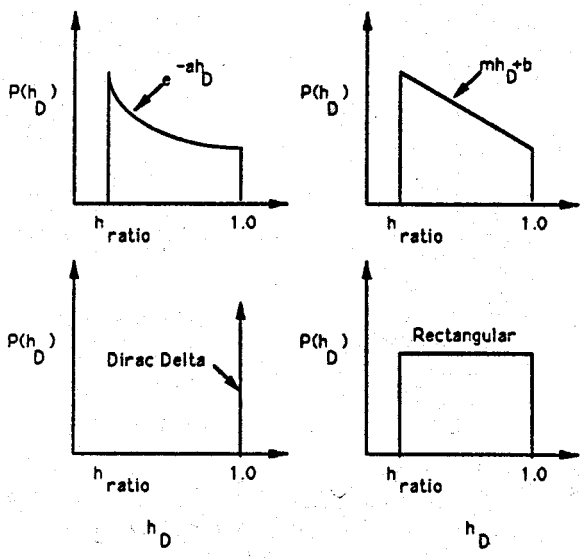

Figure 3: Probability Density Functions.

The intercept 'b' is given by:

$$b = \frac{1 - .5m + .5h_{ratio}^2}{1 - h_{ratio}}. \tag{15}$$

When 'm' is zero (linear) or 'a' is zero (exponential), both probability density functions reduce to the rectangular distribution:

$$P(h_D) = \frac{1}{1 - h_{ratio}}, \tag{16}$$

and when 'm' or 'a' approach infinity, the solutions reduce to the Dirac delta function:

$$P(h_D) = \delta(h - H). \tag{17}$$

The Dirac delta function is zero when $h \neq H$ and infinite when $h = H$ where H is the characteristic length of all matrix blocks. The Dirac delta distribution describes fractures that are perfectly ordered as in the Warren and Root model. The rectangular distribution, however, represents a continuum of block sizes that are equally probable from the smallest (h_{min}) to the largest (h_{max}). In general, the rectangular distribution should be used if the distribution type is unknown.

Once the type of PDF is determined, Equation 11 can be solved for f(s). Table 1 lists the solutions of f(s) for the various PDF's.

DISCUSSION-DRAWDOWN TESTING

Equation 4 in the absence of wellbore storage and skin reduces to:

$$\bar{P}_{D_w} = \frac{K_0(\sqrt{sf(s)})}{s^{3/2}\sqrt{f(s)}K_1(\sqrt{sf(s)})}. \tag{18}$$

Equation 18 is evaluated for the exponential PDF listed in Table 1. Figure 4 illustrates the response for varying values of 'a' holding h_{ratio} constant. For positively increasing

PDF	f(s), where $\xi = \sqrt{\frac{sm_f L^2}{\lambda_{max}}}$
Exponential	$\omega_f + \frac{a\omega_m}{\xi(e^{-ah_{ratio}} - e^{-a})} \int_{(h_{ratio})}^{\xi} \frac{e^{\frac{-ay}{\xi}} tanh(y)}{y[1 + S_{ID_{max}} \xi\, tanh(y)]} dy$
Linear	$\omega_f + \frac{\omega_m}{\xi[.5m(1 - h_{ratio}^2) + b(1 - h_{ratio})]} \int_{(h_{ratio})}^{\xi} \frac{[\frac{m}{\xi} + \frac{b}{y}] tanh(y)}{1 + S_{ID_{max}} \xi\, tanh(y)} dy$
Rectangular	$\omega_f + \frac{\omega_m}{\xi(1 - h_{ratio})} \int_{(h_{ratio})}^{\xi} \frac{tanh(y)}{y[1 + S_{ID_{max}} \xi\, tanh(y)]} dy$
Dirac delta	$\omega_f + \frac{\omega_m tanh(\xi)}{\xi[1 + S_{ID} \xi tanh(\xi)]}$, where $\lambda_{min} = \lambda_{max} = \lambda$

Table 1: Functions f(s) for various PDF's.

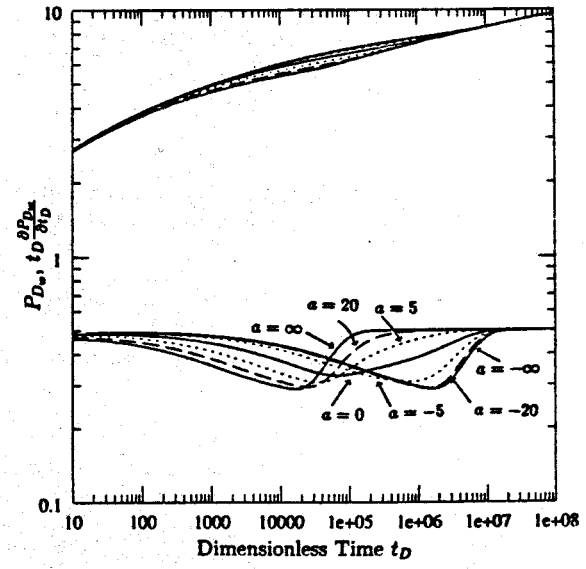

Figure 4: Exponential PDF: Varying 'a' with $h_{ratio} = .1$, $\lambda_{min} = 10^{-7}$, $\omega_m = .9$.

values of 'a', fracture intensity decreases and the response approaches the Dirac delta response for a uniform matrix block size h_{max}. For negatively increasing values of 'a', fracture intensity increases and the response approaches the Dirac delta response for a uniform matrix block size h_{min}.

For 'a' = 0, the response is that of a rectangular distribution of matrix block sizes. Also, it is evident the derivative profile shows a substantial degree of asymmetry with respect to the time axis as 'a' increases or decreases to large values. The response for the rectangular matrix block size distribution, however, is nearly symmetric. Asymmetry increases as fracturing becomes more uniform. Therefore, the shape of the derivative profile can be used as a qualitative indicator of the degree of matrix block size variability or nonuniformity. In addition, the parameter h_{ratio} is important in estimating matrix block size variability. An h_{ratio} approaching one indicates perfectly uniform fracturing, while h_{ratio} approaching zero indicates perfectly nonuniform fracturing.

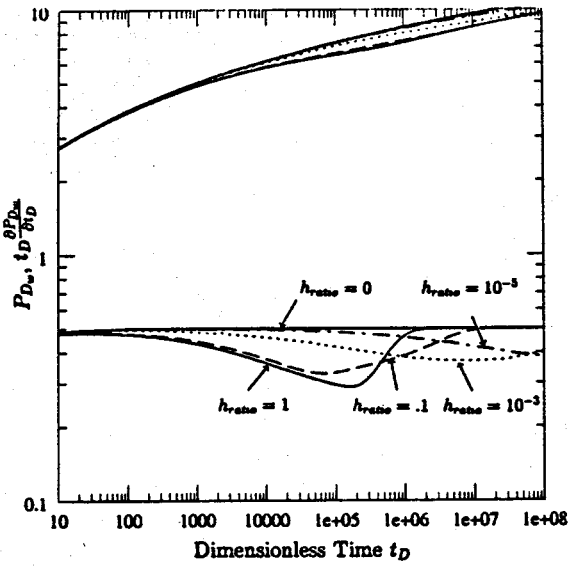

Figure 5: Rectangular PDF: Varying h_{ratio} for Geometric Mean $\lambda = 10^{-6}$, $\omega_m = .9$.

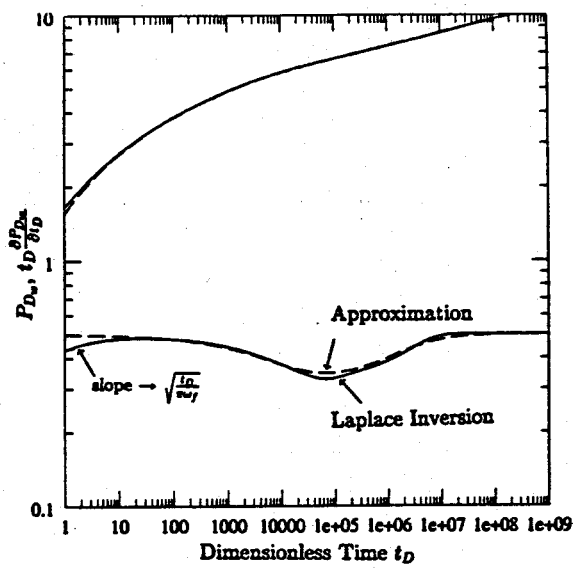

Figure 6: Rectangular PDF: Solution by Stehfest Inversion versus Time Domain Approximation, $h_{ratio} = .1$, $\lambda_{min} = 10^{-7}$, $\omega_m = .9$.

Figure 5 illustrates the pressure response for varying values of h_{ratio} with 'a' held constant. For h_{ratio} equal to zero, the response is similar to that of a homogenous reservoir. This occurs because there is an incessant gradual contribution from the matrix to the fractures. As long as fracturing is extremely nonuniform, the response will not exhibit the classical profile of a distinct transition zone separating early and late time response. For the rectangular PDF, a type curve can be developed for estimation of ω_m, λ_{min}, and h_{ratio}. The type curve is generated using the following time domain solution of the wellbore pressure response:

$$P_{D_w} = \frac{1}{2}[ln(\frac{t_D}{F(t_D)r_D^2}) + .80907], \qquad (19)$$

where $F(t_D)$ is the time-dependent reservoir storativity:

$$F(t_D) = \omega_f + \omega_m \int_{h_{ratio}}^{1} \sqrt{\frac{\lambda\gamma t_D}{\omega_m}} tanh(\sqrt{\frac{\omega_m}{\lambda\gamma t_D}}) P(h_D)\, dh_D . \qquad (20)$$

Equations 19 and 20 are obtained by applying the inversion technique of Najurieta and Schapery [17,15,14]. For the rectangular PDF, Equation 20 becomes:

$$F(\frac{t_D}{\tau_{max}}) = \omega_f + \frac{\omega_m}{(1-h_{ratio})}\sqrt{\frac{t_D}{\tau_{max}}} \times \int_{h_{ratio}\sqrt{\frac{\tau_{max}}{t_D}}}^{\sqrt{\frac{\tau_{max}}{t_D}}} \frac{tanh(y)}{y}\, dy, \qquad (21)$$

where y is the variable of integration and τ is the matrix response time coefficient:

$$\tau = \frac{\omega_m}{\gamma\lambda}, \qquad (22)$$

and τ_{max} is the response time coefficient of the most dormant or largest matrix block:

$$\tau_{max} = \frac{\omega_m}{\gamma\lambda_{min}}. \qquad (23)$$

In general, the time domain approximation gives remarkably good results (Figure 6). Using the difference between the extrapolated late time pressure response and the observed pressure, one obtains:

$$\Delta P = P_{D_w} - P_{D_{w_{late}}} = -\frac{1}{2} ln F(\frac{t_D}{\tau_{max}}). \qquad (24)$$

The type curve (Figure 7) is then generated by plotting the pressure difference ΔP versus $\frac{t_D}{\tau_{max}}$ for a range of h_{ratio} and ω_m values.

The type curve demonstrates several key ideas. As matrix storativity predominates (increasing ω_m), h_{ratio} affects the pressure response more significantly. The effect of an increasing h_{ratio} on the pressure response is greatest for lower values of h_{ratio} (e.g. the pressure response changes more significantly for h_{ratio} values from 0.1 to 0.5 than from 0.5 to 1.0). Therefore, the larger the matrix block size variability, the more significantly the pressure response is affected. For h_{ratio} approaching one, the response reverts to the uniformly fractured (uniform block size) case.

An example of the effect of interporosity skin ($S_{ID_{min}}$) on the pressure transient response is shown in Figure 8. For small interporosity skin factors, a significant change in the pressure derivative is seen, and thus, the effect of the matrix block size distribution is masked. The derivative profile becomes symmetric which is typical of the PSS response demonstrated by Warren and Root. As interporosity skin increases, the derivative profile shifts in time, giving apparent λ values that are too small (more dormant). Thus, interpreting pressure transient tests via Warren and Root may give systematically lower estimates of λ than actually exists in the reservoir. The fracture intensity will then be underestimated.

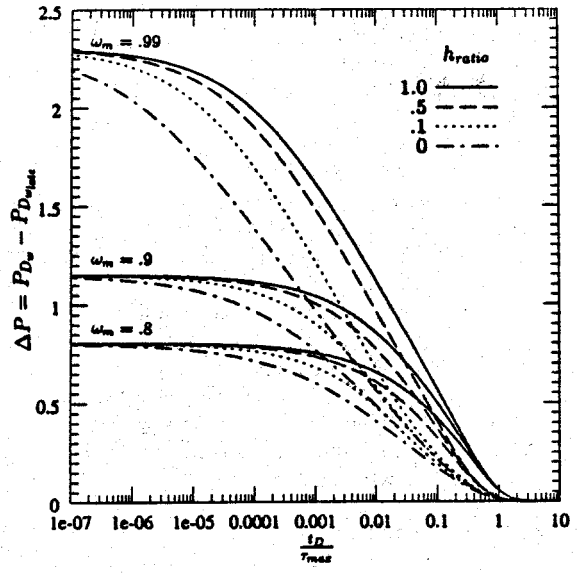

Figure 7: Rectangular PDF: Drawdown Type Curve for $t_D > 100$ and $\lambda_{min} < 10^{-4}$ for Varying h_{ratio}, λ_{min}, ω_m.

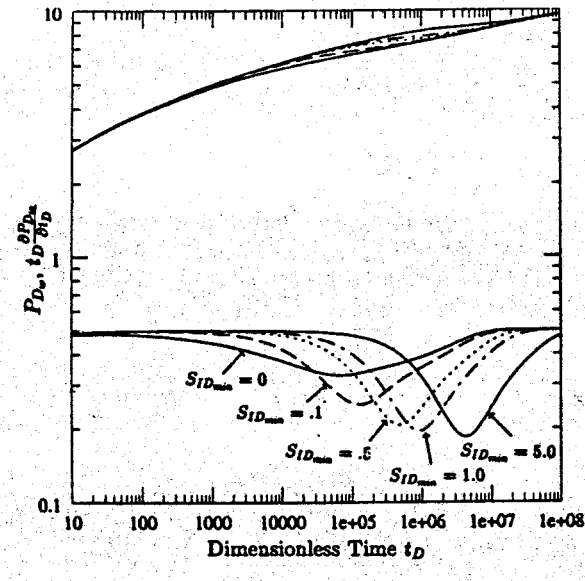

Figure 8: Rectangular PDF: Effect of Interporosity Skin, $h_{ratio} = .1$, $\lambda_{min} = 10^{-7}$, $\omega_m = .9$.

DISCUSSION-INTERFERENCE TESTING

Braester[4] demonstrated that drawdown (or buildup) testing in naturally fractured reservoirs may not be influenced by matrix blocks significantly away from the wellbore. Interference testing, therefore, is preferred because the response is affected by matrix blocks between the active and observation wells. A simplified solution for interference testing in the absence of storage and wellbore skin is the line source solution:

$$\overline{P}_{D_f} = \frac{K_0(r_D\sqrt{sf(s)})}{s}. \tag{25}$$

For any PDF distribution, it can be shown that $\theta = \lambda_{min} r_D^2$ is a correlating parameter [6,7]. For instance, using the linear PDF:

$$f(sr_D^2) = \omega_f + \frac{\omega_m}{.5m(1-h_{ratio}^2)+b(1-h_{ratio})}\sqrt{\frac{\theta}{\omega_m sr_D^2}} \times \int_{h_{ratio}\sqrt{\frac{\omega_m sr_D^2}{s}}}^{\sqrt{\frac{\omega_m sr_D^2}{s}}} [m\sqrt{\frac{\theta}{\omega_m sr_D^2}} + \frac{b}{y}]tanh(y)\,dy. \tag{26}$$

Equation 25 can then be evaluated using the inverse Laplace transform relation:

$$\mathcal{L}^{-1}[\overline{P}_{D_f}(sr_D^2)] = \frac{1}{r_D^2} P_{D_f}(\frac{t_D}{r_D^2}). \tag{27}$$

A type curve (Figure 9) is prepared using the uniform PDF case for a given ω_m. For each value of θ, h_{ratio} is varied from zero to one. If h_{ratio} determined from the type curve is equal to one, the PDF type is Dirac delta and the type curve is similar to that presented by Deruyck *et al* [6,7]. For large values of θ, the matrix block size variability becomes increasingly important and h_{ratio} can be better estimated. Thus, if the dimensionless distance (r_D) between the active and observation wells becomes large, or if λ_{min} becomes large, the matrix block size variability becomes one of the key parameters in interpretating the interference pressure transient test. For extremely large values of θ, however, the fracture response may not be detected and the response will be the same as the line source solution. Also, for large values of ω_m, the parameter h_{ratio} increasingly dominates the pressure response.

CONCLUSIONS

- A formulation incorporating transient interporosity flow and interporosity skin is presented for fractured reservoirs with variable matrix block size. Geologically realistic PDF's have been used to represent intensely or sparsely fractured reservoirs.
- Type curves have been generated for both drawdown and interference well tests based on the rectangular PDF and slab matrix block geometry. Type curves yield estimates of the parameter h_{ratio} which

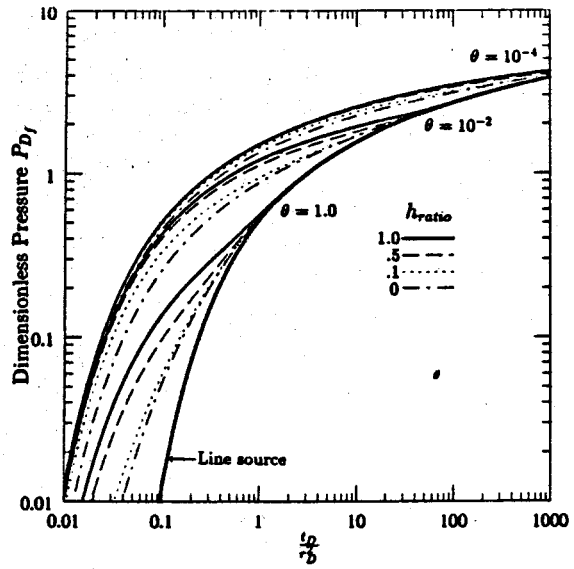

Figure 9: Rectangular PDF: Interference Type Curve for Varying h_{ratio}, θ, with $\omega_m = .9$.

describes the matrix block size variability or the degree of uniformity of fracturing. For h_{ratio} approaching unity, the response approaches that of a uniformly fractured reservoir, while for h_{ratio} approaching zero, the response resembles that of a homogeneous reservoir.

- For naturally fractured reservoirs with interporosity skin, the matrix block size variability is not estimatable. Fracture intensity may be underestimated if the Warren and Root interpretation is employed.

NOMENCLATURE

a	= exponential PDF constant
b	= intercept of linear PDF
c_f	= fracture total compressibility
c_m	= matrix total compressibility
C_D	= dimensionless wellbore storage
P(h)	= block size distribution function
$P(h_D)$	= dimensionless block size distribution function
f(s)	= Laplace space function
h	= matrix block size characteristic length (Volume/Area)
h_D	= dimensionless matrix block size length
h_f	= fracture thickness
h_{min}	= minimum block size length
h_{max}	= maximum block size length
h_{ratio}	= ratio of h_{min} to h_{max}
h_s	= interporosity damaged zone thickness
H	= constant matrix block size
k_f	= fracture permeability
k_m	= matrix permeability
k_s	= interporosity damaged zone permeability
$K_0(x)$	= modified Bessel function, second kind, zero order
$K_1(x)$	= modified Bessel function, second kind, first order
m	= slope of linear PDF
P_{D_f}	= dimensionless fracture pressure
P_{D_m}	= dimensionless matrix pressure
P_{D_w}	= dimensionless wellbore pressure
P_f	= fracture fluid pressure
P_i	= initial reservoir pressure
P_m	= matrix fluid pressure
P_w	= wellbore fluid pressure
Q(h)	= flow contribution from matrix size
r	= radial coordinate
r_D	= dimensionless radial coordinate
r_w	= wellbore radius
s	= Laplace parameter
S_D	= dimensionless wellbore skin factor
S_{ID}	= dimensionless interporosity skin factor
$S_{ID_{min}}$	= minimum dimensionless interporosity skin factor
t	= time
t_D	= dimensionless time
γ	= 1.781, exponential of Euler's constant
λ	= dimensionless interporosity flow coefficient
λ_{max}	= maximum dimensionless interporosity flow coefficient
λ_{min}	= minimum dimensionless interporosity flow coefficient
τ	= dimensionless matrix response time coefficient
τ_{max}	= maximum dimensionless matrix response time coefficient
μ	= viscosity
ϵ	= coordinate normal to fracture-matrix interface
ϵ_D	= dimensionless coordinate normal to fracture-matrix interface
ϕ_f	= dimensionless fracture porosity
ϕ_m	= dimensionless matrix porosity
ω_f	= dimensionless fracture storativity ratio
ω_m	= dimensionless matrix storativity ratio
θ	= dimensionless correlation parameter

APPENDIX

The dimensionless boundary conditions and flow equations are:

$$\frac{\partial^2 P_{D_f}}{\partial r_D^2} + \frac{1}{r_D}\frac{\partial P_{D_f}}{\partial r_D} = \omega_f \frac{\partial P_{D_f}}{\partial t_D} - \int_{h_{ratio}}^{1} \lambda \frac{\partial P_{D_m}}{\partial \epsilon_D}\Big|_{\epsilon_D=0} P(h_D)\, dh_D, \tag{28}$$

$$\frac{\partial^2 P_{D_m}}{\partial \epsilon_D^2} = \frac{\omega_m}{\lambda}\frac{\partial P_{D_m}}{\partial t_D}. \tag{29}$$

- $P_{D_f} = P_{D_m} = 0$ at $t_D = 0$
- $P_{D_f} = P_{D_m} = 0$ at $r_D \to \infty$
- $C_D \frac{\partial P_{D_w}}{\partial t_D} - \frac{\partial P_{D_f}}{\partial r_D}\Big|_{r_D=1} = 1$
- $P_{D_w} = [P_{D_f} - S_D \frac{\partial P_{D_f}}{\partial r_D}]\Big|_{r_D=1}$

- $P_{D_f} = [P_{D_m} - S_{ID}\frac{\partial P_{D_m}}{\partial \epsilon_D}]\,|_{\epsilon_D \approx 0 \text{ for slabs}}$
- $\frac{\partial P_{D_m}}{\partial \epsilon_D}\,|_{\epsilon_D \approx 1 \text{ for slabs}} = 0$ at no flow boundaries

where:

$$P_{D_f} = \frac{2\pi k_f h_f (P_i - P_f)}{q\mu} \tag{30}$$

$$P_{D_m} = \frac{2\pi k_f h_f (P_i - P_m)}{q\mu} \tag{31}$$

$$P_{D_w} = \frac{2\pi k_f h_f (P_i - P_w)}{q\mu} \tag{32}$$

$$t_D = \frac{k_f t}{(\phi_f c_f + \phi_m c_m)\mu r_w^2} \tag{33}$$

$$r_D = \frac{r}{r_w} \tag{34}$$

$$C_D = \frac{C}{2\pi h_f c_t r_w^2} \tag{35}$$

$$\lambda = \frac{k_m r_w^2}{k_f h^2} \tag{36}$$

$$\lambda_{min} = \frac{k_m r_w^2}{k_f h_{max}^2} \tag{37}$$

$$\lambda_{max} = \frac{k_m r_w^2}{k_f h_{min}^2} \tag{38}$$

$$\omega_m = \frac{\phi_m c_m}{\phi_f c_f + \phi_m c_m} \tag{39}$$

$$\omega_f = 1 - \omega_m \tag{40}$$

$$h_D = \frac{h}{h_{max}} \tag{41}$$

$$\epsilon_D = \frac{\epsilon}{h} \tag{42}$$

$$P(h_D) = h_{max} P(h)\,. \tag{43}$$

Other matrix block geometries can be included in the solution by changing the interporosity boundary conditions. After applying Laplace transforms to the flow equations and boundary conditions one obtains the solutions of Equations 3 and 4.

References

[1] Aguilera, R.:, *Naturally Fractured Reservoirs*, Petroleum Publishing Co. Tulsa, OK, (1980).

[2] Belani, A.K. and Jalali-Yazdi, Y.:, *"Estimation of Matrix Block Size Distribution in Naturally Fractured Reservoirs"*, SPE 18171, presented at the 63rd Fall Technical Conference held in, Houston, TX, Oct., 1988.

[3] Bles, J.L. and Feuga, B.:, *The Fracture of Rocks*, North Oxford Academic Publishers, (1986).

[4] Braester, C.:, *"Influence of Block Size on the Transition Curve for a Drawdown Test in a Naturally Fractured Reservoir"*, *Soc. Pet. Eng. J.*, 498–504, (1984).

[5] Cinco-Ley, H., et al.:, *"The Pressure Transient Behavior for Naturally Fractured Reservoirs with Multiple Block Size"*, SPE 14168, presented at the 60th Fall Technical Conference held in, Las Vegas, NV, Sept., 1985.

[6] Deruyck, B.G.:, *Interference Well Test Analysis For A Naturally Fractured Reservoir*, Master's thesis, Stanford Univ., (June 1980).

[7] Deruyck, B.G., et al.:, *"Interpretation of Interference Tests in Reservoirs with Double Porosity Behavior-Theory and Field Examples"*, SPE 11025, presented at the 57th Fall Technical Conference held in, New Orleans, LA, Sept., 1982.

[8] Dyer, J.R.:, *Jointing in Sandstones, Arches National Park, Utah*, PhD thesis, Stanford Univ., (August 1983).

[9] Isaacs, C.M.:, *"Geology and Physical Properties of the Monterey Formation, California"*, SPE 12733, presented at the California Regional Meeting held in, Long Beach, April, 1984.

[10] Johns, R.T. and Jalali-Yazdi, Y.:, *"Comparison of Pressure Transient Response in Intensely and Sparsely Fractured Reservoirs"*, SPE 18800, presented at the Calif. Reg. Mtg. held in, Bakersfield, CA, April, 1989.

[11] Mattax, C.C. and Kyte, J.R.:, *"Imbibition Oil Recovery from Fractured, Water-Drive Reservoir"*, *Soc. Pet. Eng.*, 177–184, (June 1962).

[12] McQuillan, H.:, *"Small Scale Fracture Density in Asmari Formation of Southwest Iran and its Relation to Bed Thickness"*, *AAPG Bulletin*, 57(12):2367–2385, (Dec. 1973).

[13] Moench, A.F.:, *"Double-Porosity Models for a Fissured Groundwater Reservoir with Fracture Skin"*, *J. Water Resources*, 20(7):831–846, (July 1984).

[14] Najurieta, H.L.:, *"Interference and Pulse Testing in Uniformly Fractured Reservoirs"*, SPE 8283, presented at the 54th Fall Technical Conference held in, Las Vegas, NV, Sept., 1979.

[15] Najurieta, H.L.:, *"A Theory for Pressure Transient Analysis in Naturally Fractured Reservoirs"*, *J. Pet. Tech.*, 1241–1250, (July 1980).

[16] Pollard, D.D. and Aydin, A.:, *"Progress in Understanding Jointing Over the Past Century"*, *Geol. Soc. Amer. Bull.-Centennial Vol.*, (March 1988).

[17] Schapery, A.:, *Approximate Methods of Transform Inversion for Viscoelastic Stress Analysis*, Technical Report, 4th U.S. National Congress Appl. Math., (1961).

[18] Segall, P.:, *The Development of Joints and Faults*, PhD thesis, Stanford Univ., (July 1981).

[19] Warren, J.E. and Root, P.J.:, *"The Behavior of Naturally Fractured Reservoirs"*, *Soc. Pet. Eng. J.*, 245–55, (Sept. 1963).